In-Situ Neutral Density and Wind Measurements from the APEP Eclipse Rocket Campaign

Nathan Graves(gravesn@my.erau.edu)[1], Aroh Barjatya[1], Robert Clayton[1], Henry Valentine[1], Joshua Milford[1]
Kenneth Obenberger[2], Jeffrey Holmes[2], Jorge (Koki) Chau[3], Sebastijan Mrak[4], and Gerald Lehmacher[5]
(1) Embry-Riddle Aeronautical University, Daytona Beach, FL (2) Air Force Research Lab, Albuquerque, NM (3) Leibnitz Institute of Atmospheric Physics, Kuhlungsborn, Germany (4) JHU Applied Physics Laboratory, Maryland (5) *Clemson University, Clemson, South Carolina*

SAIL Space and Atmospheric Instrumentation Lab sail.erau.edu

Abstract

Atmospheric **P**erturbations around **E**clipse **P**ath (**APEP**) is a sounding rocket campaign to study the electrodynamics of Earth's ionosphere during the October 2023 annular eclipse and the April 2024 total eclipse in the United States. The launch salvo during each eclipse consists of three launches: one prior to the peak local eclipse, one during the peak local eclipse, and one after the peak local eclipse. Each rocket is equipped with a suite of instruments to conduct in-situ measurements of the plasma/neutral environment and fully characterizes its associated electrodynamics and neutral dynamics. For neutral dynamics, the main payload carried two ionization gauges for measurements throughout the flight and a sensitive accelerometer for drag-based measurements up to 110km. Additionally, four ejectable subpayloads carried accelerometers for distributed drag-based neutral density measurement. This work presents preliminary results showing in-situ observations of neutral winds and neutral dynamics throughout both the eclipses using low-cost ionization gauges and accelerometers.

APEP Mission Overview

Mission Objective

First simultaneous multipoint in-situ observations of electrodynamics and neutral dynamics during solar eclipses.

Method

Launch instrumentation aboard sounding rockets before, during, and after the 2023 annular eclipse and the 2024 total eclipse from rocket ranges near the path of eclipse.

Instrumentation Suite

- Ion Gauge (IG)
- Magnetometer (MAG)
- Electric Field Probes (EFP)
- Accelerometer (ACC)
- Ejectables (3× **ROB**, 1 × RPA)
- Fixed/Sweeping Langmuir Probes (**mNLP**, **PIP**, SLP)

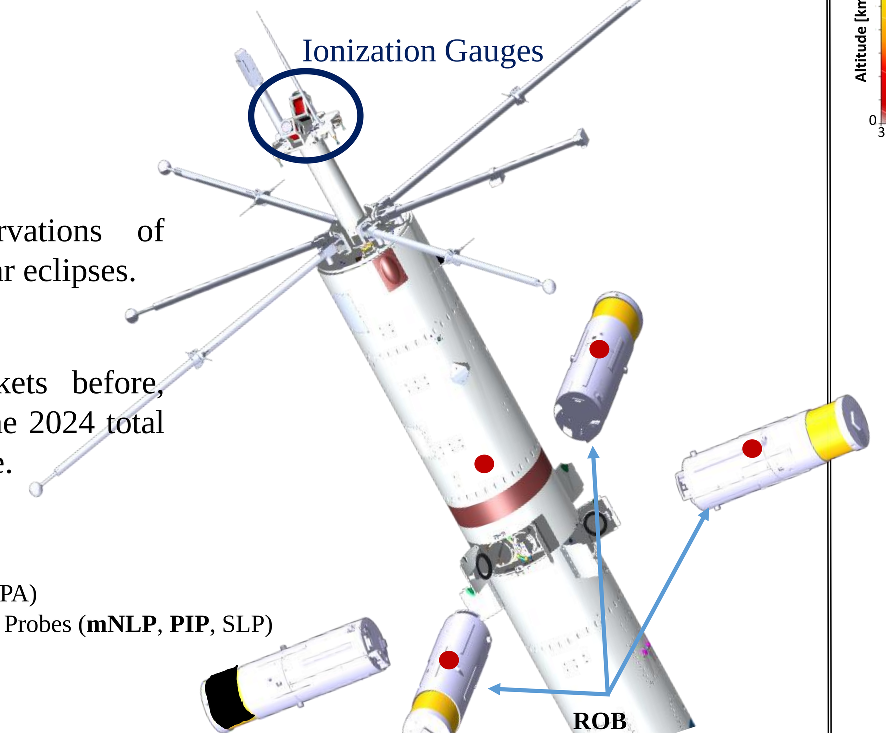

Figure 1: APEP Sound Rocket Payload

Launch Details

	APEP 1 - WSMR Oct 14, 2023 - Annular Eclipse			APEP 2 - WFF Apr 08, 2024 - Total Eclipse		
	Rocket #	T_{Launch}	Δt Peak	Rocket #	T_{Launch}	Δt Peak
Pre-Eclipse	36.386	10:00 MDT	-35 min	36.392	14:40 EDT	-45 min
Peak-Eclipse	36.387	10:35 MDT	0 min	36.393	15:25 EDT	0 min
Post-Eclipse	36.388	11:10 MDT	+35 min	36.394	16:28 EDT	+63 min

Table 1: APEP launch details

Figure 2: Eclipse paths and launch sites

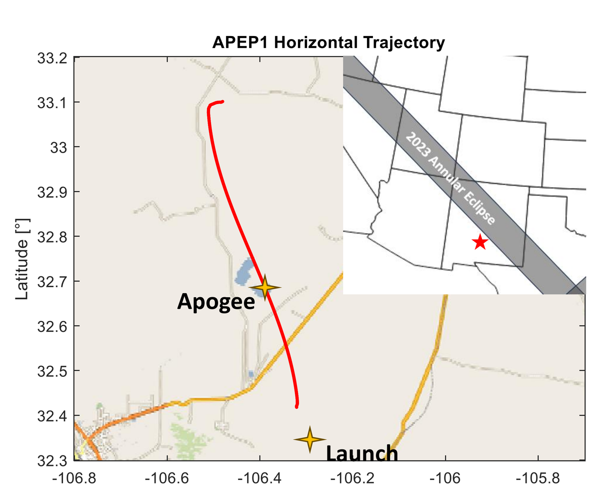

Figure 3: APEP1 main payload horizontal trajectory

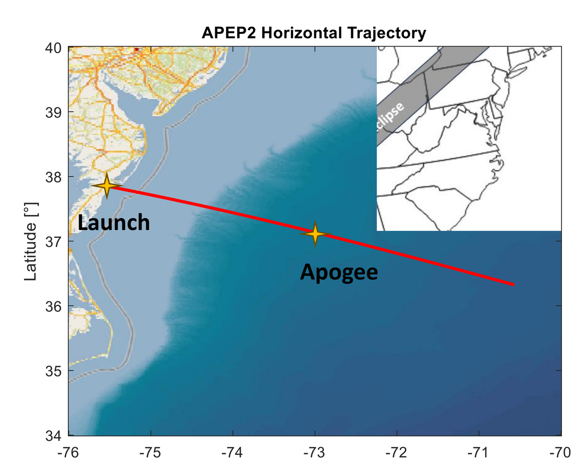

Figure 4: APEP2 main payload horizontal trajectory

Instruments

Pirani/Cold Cathode Ionization Gauge [6]

Pfeiffer PKR360 x 2
- Mounted 45° from axial aft end on the main payload
- Measurement range: 7.5e-10 to 750 torr
- 5kHz measurement frequency
- 5% Repeatability
- Calibrated at Clemson University

ADXL 355 [7]
- 1x Centrally located on main payload,
- 4x on subpayloads
- ±2g measurement range
- ~30 µg resolution
- 0.25 - 2.5 kHz measurement frequency

PKR360 Ionization Gauge Sensor

Since the ionization gauge on the rocket is moving through the atmosphere at a high velocity, the measured density will be enhanced over the true value by a "ram factor". Assuming free molecular flow this factor can be calculated with equation (2) where α is the angle of attack to the ram direction, T_1 is the neutral temperature, T_2 is the temperature within the gauge, and $\bar{m}$ is the mean molecular mass. [5][8] In the current analysis, the MSIS model temperature is used.

$$n_{meas} = RF * n_{actual} \quad (1)$$

$$RF(S) = \sqrt{\frac{T_1}{T_2}} \exp(-S^2) + \sqrt{\pi}\, S\,(1 + \mathrm{erf}(S)) \quad (2)$$

$$S = \frac{v\cos(\alpha)}{\sqrt{2kT_1/\bar{m}}} \quad (3)$$

Accelerometer measurements can be converted to density by solving the drag equation for mass density. Drag coefficients can be drawn from simulation or experiment. [9]

$$a_{drag} = C_d \frac{\rho\, v^2}{2m} A_{proj} \quad (4); \qquad \rho = \frac{2m\, a_{drag}}{C_d\, A_{proj}\, v^2} \quad (5)$$

APEP 1 : Oct 14, 2023 Annular Eclipse

Launch Conditions

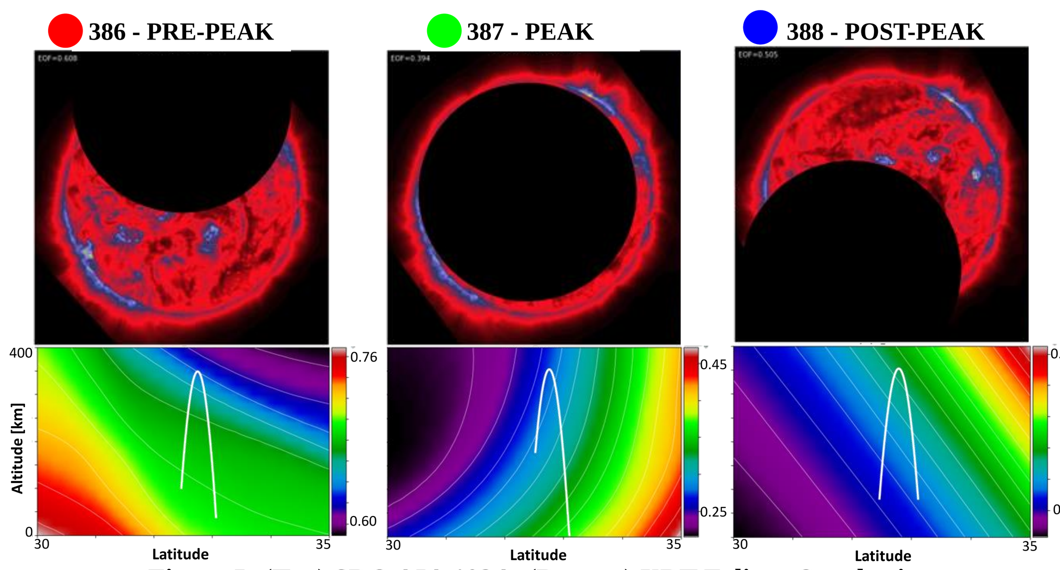

Figure 5: (Top) SDO AIA 193A. (Bottom) XRT Eclipse Occultation.

Launch timing was based on solar occultation. Note the delay in the F region response.

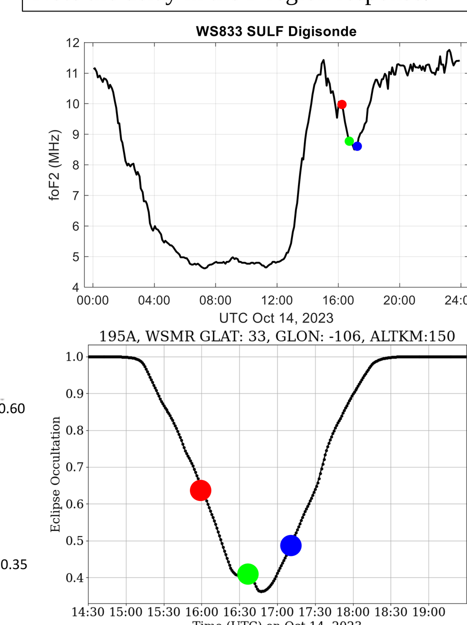

Figure 6: (Top) WSMR digisonde (Bottom) Occultation Timeline

Flight Data

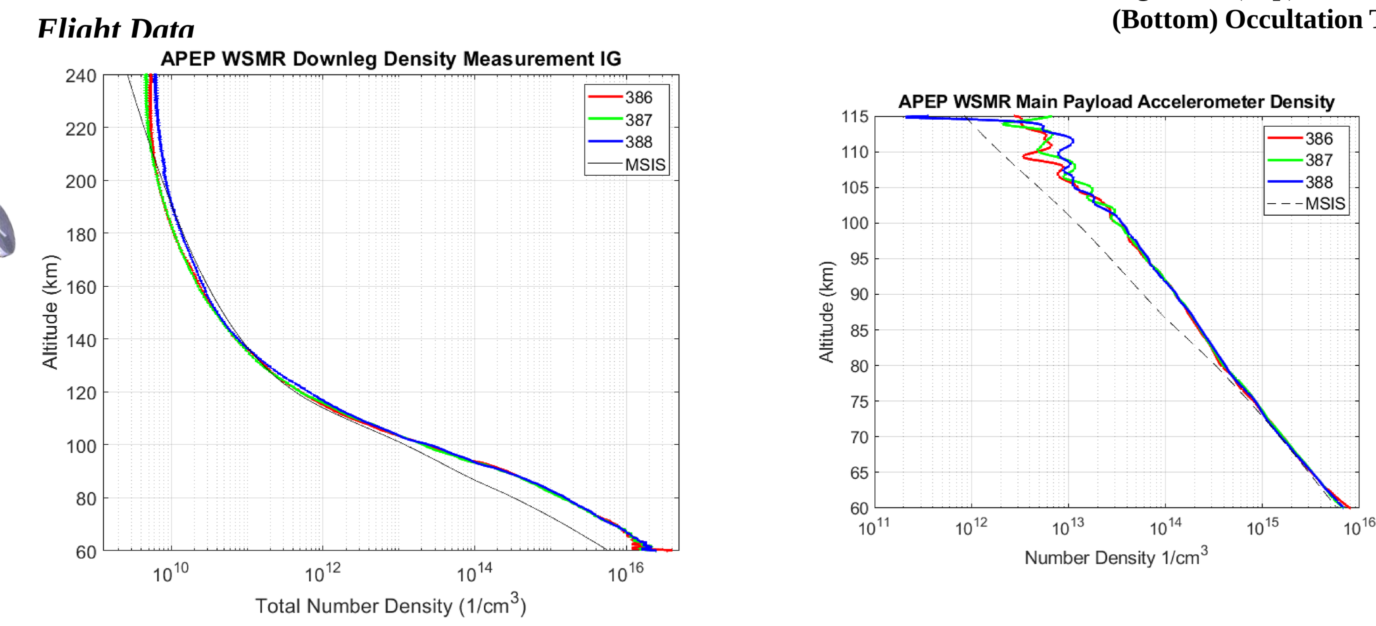

Figure 7: (Left) Ionization gauge derived number densities for the annular eclipse campaign. (Right) Drag-derived number densities. Plotted with NRLMSIS2.0

Observed Dynamics – Neutral Winds

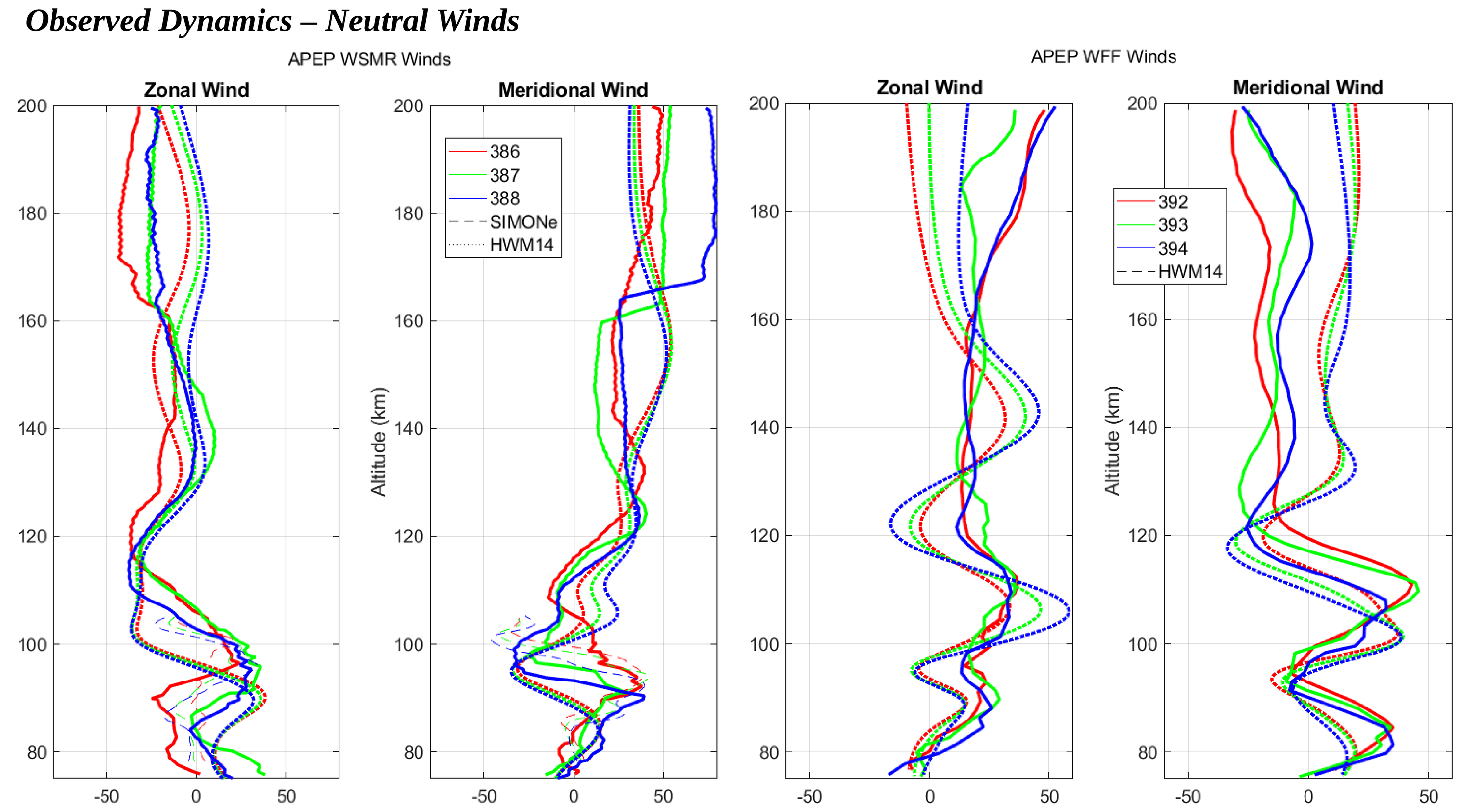

Figure 11: Horizontal neutral wind measurements from each rocket, plotted with the horizontal wind model HWM14

Figure 11 shows the derived neutral wind estimates for both campaigns, compared with the HWM14 [1], and for the annular eclipse, a supporting SIMONe Specular Meteor Radar. The wind vector is derived by calculating the residual pressure difference from the average observed by the gauge as it rotates with the rocket. Assuming vertical wind is zero, the remaining signal is due to horizontal wind and the projection of the rocket velocity on the spin plane. The orientation of the gauge at peak signal is opposite the direction of net wind, and magnitude can be estimated by numerically solving Equation (2) for *v*. While this process is still being evaluated and improved, we have high confidence because in the mutually operating range, the ionization gauge winds track with the radar derived winds, showing the decrease in the meridional wind shear altitude around 100km. Additionally, the winds in the 100-120km range are associated with Sq currents observed by the magnetometer instrument (below), and the steep gradient at 160km in the WSMR meridional wind is associated with plasma irregularities (see poster ITMA-2).

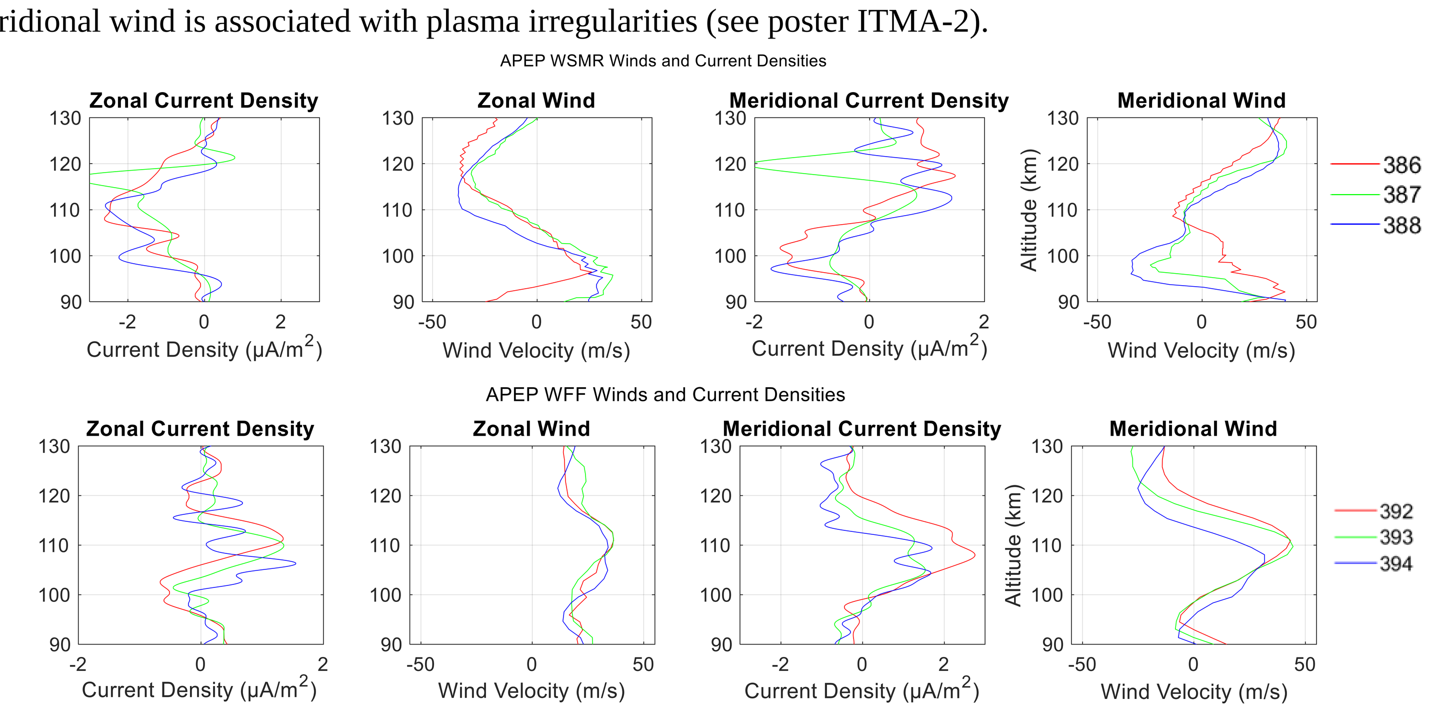

Figure 12: Zonal and Meridional Winds and Magnetometer-derived current densities. Note the decrease in wind speed and current density in the meridional component from pre to post-eclipse measured by APEP WFF.

APEP 2 : Apr 08, 2024 Total Eclipse

Launch Conditions

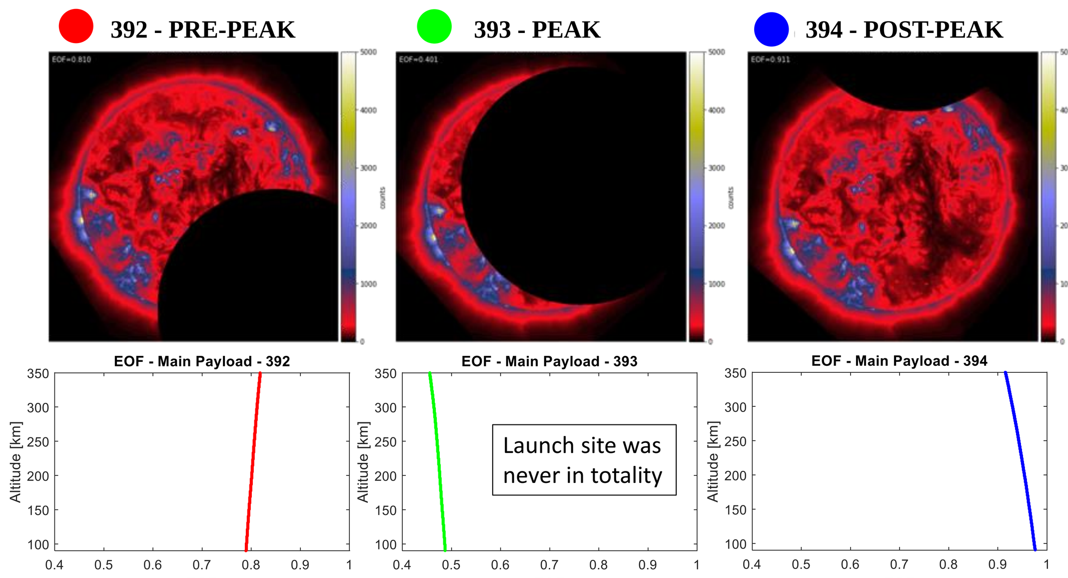

Figure 8: (Top) SDO AIA 193A [2]. (Bottom) 193Å Eclipse Occultation.

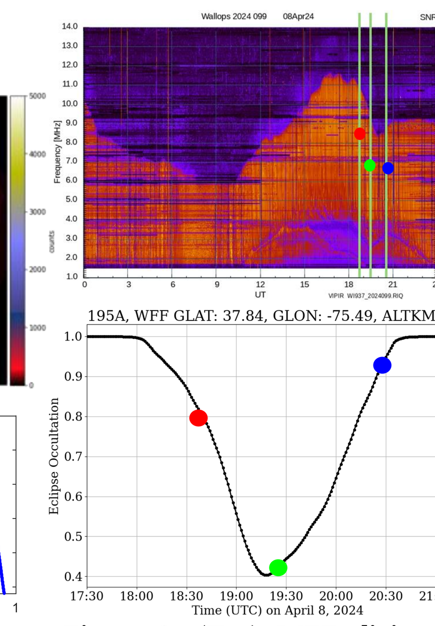

Figure 9: (Top) WFF digisonde (Bottom) Occultation Timeline

Flight Data

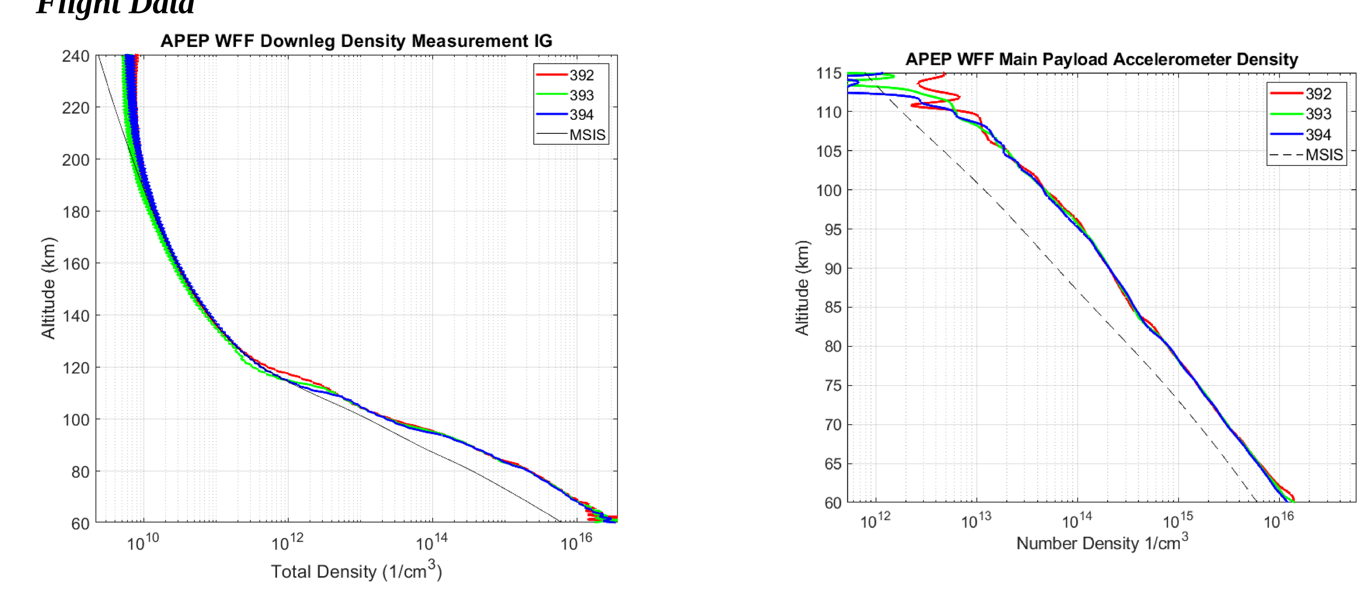

Figure 10: (Left) Ionization gauge derived number densities during the total eclipse campaign. (Right) Drag-derived number densities. Plotted with NRLMSIS2.0

Observed Dynamics – Relative Density

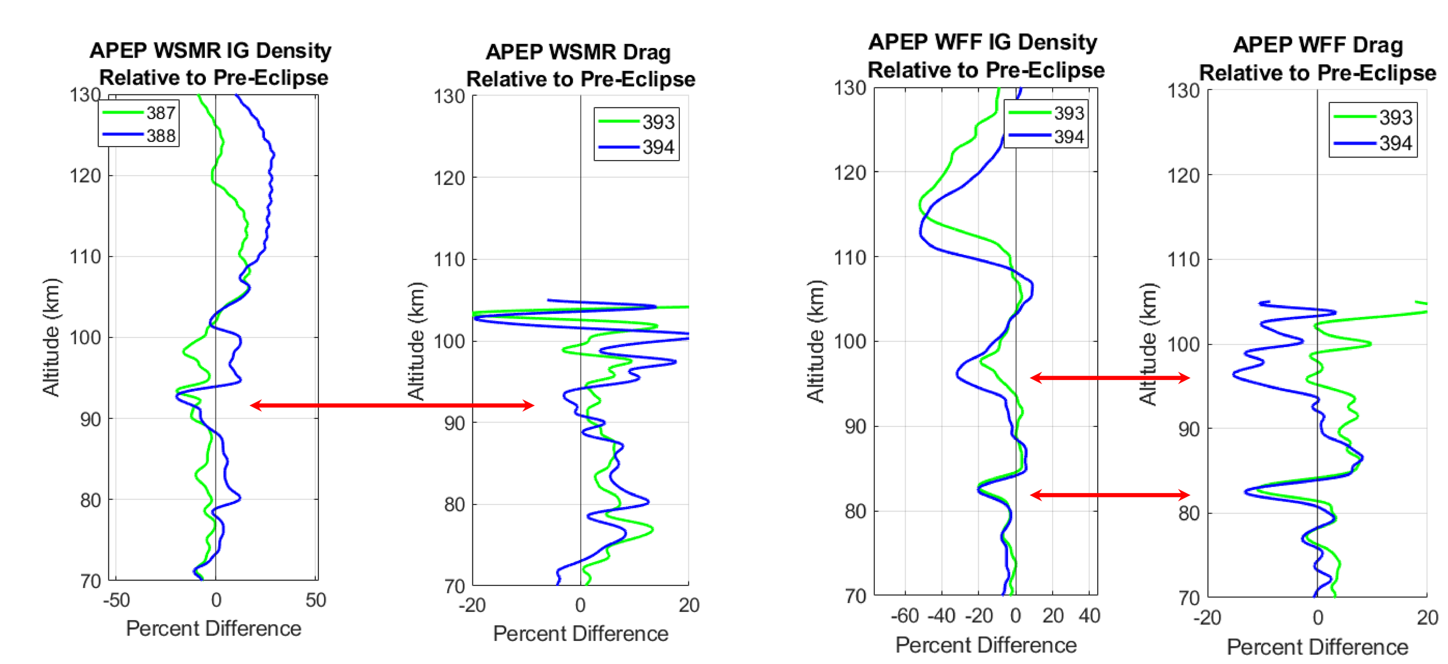

Figure 13: Density changes relative to the pre-eclipse rocket flight for each campaign and instrument.

Figure 13 shows the relative density changes with respect to the first rocket flight before each eclipse, compared with the changes in the acceleration due to drag. In each campaign, relative decreases in density are observed at similar altitudes in both measurements. However, the decreases during the total eclipse mission were larger, possibly due to a larger time difference between launches and effects of typical diurnal tides at that local time.

Takeaways and Future Work

- The flight performance of ***low-cost accelerometers and ionization gauges*** to measure neutral density has been demonstrated and show agreement with relative density change flight to flight within their mutually operating range.
- Ionization gauge measurements have been used to derive ***neutral winds between 75-200km*** and observe similar features to the meteor radar, showing the altitude changes in the shear at 100km. However, further analysis with Direct Simulation Monte-Carlo (DSMC) free molecular flow simulations is required to assess and include an error-bar in wind magnitude.
- Additional analysis of drag data will be performed in order to estimate winds below 110km, providing corroborating measurements to the ionization gauge derived winds.

References

[1] D. P. Drob et al., "An update to the Horizontal Wind Model (HWM): The quiet time thermosphere," Earth and Space Science, vol. 2, no. 7. American Geophysical Union (AGU), pp. 301–319, Jul. 2015. doi: 10.1002/2014ea000089.

[2] J. T. Emmert et al., "NRLMSIS 2.0: A Whole-Atmosphere Empirical Model of Temperature and Neutral Species Densities," Earth and Space Science, vol. 8, no. 3. American Geophysical Union (AGU), Mar. 2021. doi: 10.1029/2020ea001321.

[3] Offermann, D., 1974. Composition variations in the lower thermosphere. Journal of Geo Research 79, 4281-4293.

[4] Lehmacher G.A., Gaulden T.M. Larsen M.F., Craven J.D., Multiple neutral density measurements in the lower thermosphere with cold-cathode ionization gauges, Journal of Atmospheric and Solar-Terrestrial Physics, Volume 92, 2013, Pages 137-144, ISSN 1364-6826, https://doi.org/10.1016/j.jastp.2012.11.002.

[5] Lehmacher, G., *et. al.*, On the Short-term Variability of Turbulence and Temperature in the Winter Mesosphere. *Annales Geophysicae* **36,** 4 (2018). DOI: 10.5194/angeo-36-1099-2018

[6] Pfeiffer Vacuum, https://www.pfeiffer-vacuum.com/en/

[7] Analog Devices, https://www.analog.com/en/products/adxl355.html

[8] Patterson, G.N., 1956. Molecular Flow of Gases. John Wiley and Sons, New York.

[9] Heddleson, C. F., et al., 1957. Summary of Drag Coefficients of Various Shaped Cylinders. DTIC ADA395503